Validation of Rigid Registration of Mammographic Images

Jelena Bozek [1], Mislav Grgic [1], Julia A. Schnabel [2]
[1] University of Zagreb, Faculty of Electrical Engineering and Computing, Zagreb, Croatia
[2] University of Oxford, Institute of Biomedical Engineering, Department of Engineering Science, Oxford, United Kingdom
jelena.bozek@fer.hr

Abstract - Mammographic image registration is an important step in the analysis of differences between the left and right breast in order to detect bilateral asymmetry, which is an early sign of breast cancer. We have used rigid registration to align left and right mammographic images as a first step for comparing corresponding regions in the left and right breast. Registration performance was tested on a dataset consisting of normal and asymmetric cases obtained from three different mammographic image databases: mini-MIAS, DDSM and our own database containing digital mammographic images. For the validation of mammographic image registration, we have used several measures: sum of squared differences (SSD), normalized cross correlation (NCC), mutual information (MI), normalized mutual information (NMI), structural similarity index (SSIM) and universal image quality (UIQI) measure. Results showed that rigid registration works well on all three databases and that it might be a good first step in analysing bilateral asymmetry.

Keywords - Mammography; Bilateral Asymmetry; Rigid Registration

I. INTRODUCTION

Bilateral asymmetry is one of the early signs that may indicate breast cancer or its future onset. Bilateral asymmetry is defined as presence of greater volume of fibroglandular tissue in one breast compared to the corresponding area in the other breast [1]. When analysing mammographic images and comparing features in the left and right breast, it is recommended to perform registration of the images [2-6]. Registration enables comparison of the corresponding regions in the left and right breast. However, registration of mammographic images is a challenging task. The mammographic imaging procedure projects 3D objects into a 2D mammographic image and introduces distortions and displacement of the breast tissue due to the compression with a paddle. Thus, some researchers proposed bilateral asymmetry analysis without registration, or using registration only in the later stage of the algorithm [7-11]. Several mammographic image registration methods have been proposed for temporal analysis of mammographic images [12-15].

Validation of breast registration methods and their accuracy is not a simple task, since the ground truth is usually not available. In [16] some of the most common methods for registration validation are mentioned, such as phantom studies, subtraction of images, calculation of the Euclidian distance between landmarks and visual inspection. Van Engeland et al. [17] compared four methods for registering temporal mammographic images. They measured the performance of tested methods by comparing the distance between annotations of abnormalities in the previous and current view before and after registration. Wirth et al. [18] evaluated rigid and non-rigid registration of temporal mammographic images using image subtraction and resulting differences before and after registration.

In this paper we have used rigid registration to align mammographic images. The main image registration steps are explained in Section II and parameters that we used for rigid registration are presented in Section III. Section IV presents the datasets used for registration. Results are presented and discussed in Section V and conclusions are given in Section VI.

II. IMAGE REGISTRATION

Registration is the process of determining a mapping between the coordinates in one space and those in another, to achieve biological, anatomical or functional correspondence. Registration techniques can be classified into feature-based and intensity-based registration techniques. Feature-based registration techniques use anatomical and geometric features in order to perform matching. Commonly used features in mammogram registration methods are landmarks such as breast boundary, nipple and pectoral muscle visible in the medio-lateral view. Intensity-based registration techniques use pixel intensity information of the two images to perform registration. These are sometimes called pixel-similarity (when registering 2-D images) or voxel-similarity (when registering 3-D images) registration techniques. Registration algorithm consists of three components: transformation model, cost function and optimization.

The transformation defines geometric mapping T from one coordinate space to another and can be expressed as

$$T : x_B \mapsto x_A \Leftrightarrow T(x_B) = x_A \,. \qquad (1)$$

Registration algorithms that make use of geometrical features in the images involve identifying features such as sets of image points $\{x_A\}$ and $\{x_B\}$ that correspond to the same physical entity visible in both images, and calculating T for these features [19]. When an intensity-based registration technique is used, the transformation T is iteratively determined by optimizing a similarity measure between the pixel intensities in the two images. At each iteration, the image is transformed using the current estimate of T and the similarity measure is recalculated.

We have used rigid registration for aligning mammographic images of the left and right breast. The rigid transformation describes translation (t_x, t_y) and rotation by an angle θ and can be expressed as

$$\begin{bmatrix} x_B \\ y_B \end{bmatrix} = \begin{bmatrix} t_x \\ t_y \end{bmatrix} + \begin{bmatrix} \cos\theta & -\sin\theta \\ \sin\theta & \cos\theta \end{bmatrix} \begin{bmatrix} x_A \\ y_A \end{bmatrix} \quad (2)$$

where coordinate (x_B, y_B) is the transformed coordinate (x_A, y_A) [20]. The rigid transformation is used to compensate global motion of the breast. It preserves the distance between all points in the object transformed.

The cost function, the second component of the registration algorithm, represents the energy of the system being modelled. It is usually a pixel (or voxel in 3D case) similarity measure. The similarity measure is calculated from the pixel intensity values in the images. The similarity measure used in this paper is the sum of squared differences (SSD) between images and is expressed by

$$SSD = \frac{1}{N} \sum \left| A(x_A) - B^T(x_B) \right|^2 \quad (3)$$

where N is the number of pixels, $A(x_A)$ and $B^T(x_B)$ are intensity values at the locations x_A in image A and x_B in the transformed image B^T, respectively. The sum of squared differences relies on the exact pixel intensity values in the image.

The third component of the registration algorithm is the optimization method which minimizes the cost function, i.e. similarity measure, in order to find the optimal transformation parameters. At each iteration, the current estimate of the transformation is used to calculate a similarity measure. The optimization algorithm then makes another estimate of the transformation, evaluates the similarity measure again, and continues until the algorithm converges, at which point no transformation can be found that results in a better value of the similarity measure, to within a preset tolerance [21]. We have used a downhill descent optimization method and a multiresolution approach [22]. The optimization algorithm can sometimes converge to a local optimum, which is not the correct solution and thus registration can fail. Some of these optima are small and can be removed from the parameter space of values of the similarity measures by blurring the images prior to registration using multiresolution approach [21]. In the multiresolution approach images are first registered at low resolution, then the transformation solution obtained at this resolution is used as the starting estimate for the registration at a higher resolution, until the original resolution level is reached.

III. METHODOLOGY

In order to register left and right mammographic images we have used rigid registration to compensate for global misalignment. We have used the Image Registration Toolkit (IRTK) which is a comprehensive library of tools for medical image registration [22]. It implements a variety of algorithms for 2D and 3D image registration, including rigid, affine and non-rigid registration that were written by Daniel Rueckert and Julia Schnabel. The rigid registration algorithm is based on the method proposed in Studholme et al. [23]. This method used a simple multiresolution hill climbing algorithm. All images were sub-sampled using a Gaussian kernel to form lower resolution versions. This produces a simple Gaussian pyramid where smaller objects are removed as blurring is increased, resulting in a smooth function of misalignment between low resolution images at the top of the pyramid. These images containing fewer, larger-size pixels can be used to provide an efficient initial registration estimate which is then refined using higher resolution images lower in the pyramid. Registration was performed at three resolution levels. Registration started at an image sampling resolution of 0.8 x 0.8 mm with an optimisation step size of 0.8 mm and terminated at a resolution of 0.2 x 0.2 mm and step size of 0.2 mm. Original resolution of our images was 0.2 x 0.2 mm. Similarity measure used was SSD and the optimization method was downhill descent.

We have used mammographic image of the right breast as the source image which was registered to the mammographic image of the left breast which was the target image.

IV. DATASET

We have used three different datasets consisting of mammographic image pairs from three different databases: publicly available mini-MIAS and DDSM with digitised mammographic images and our database KBD-FER with digital mammographic images.

The mini-MIAS (Mammographic Image Analysis Society) database [24] comprises 322 digitised images of left and right breasts in medio-lateral oblique (MLO) view. The image resolution is 0.2 x 0.2 mm and every image has 1024 × 1024 pixels. From this database we used all 15 asymmetric cases (30 mammographic images of left and right breast) available in the database and of 20 randomly selected normal cases (40 mammographic images of the left and right breast). The breast area in each image was manually segmented by a non-clinical expert to eliminate background artifacts.

The DDSM (Digital Database for Screening Mammography) [25-26] contains approximately 2500 cases of digitised mammographic images of different resolutions and size, scanned with three different scanners. Each case includes cranio-caudal (CC) and MLO views of left and right breast, i.e. four images per case. From this database we have used 38 mammographic image pairs in MLO view with bilateral asymmetry and randomly selected 20 normal mammographic image pairs in MLO view. We have reduced all images to the resolution of 0.2 x 0.2 mm and cropped/padded them so that every image is 1024 × 1024 pixels. The breast area in each image was manually segmented by a non-clinical expert to eliminate background artifacts.

The third dataset was obtained from the digital mammographic image database KBD-FER developed in cooperation with the Department of Diagnostic and Interventional Radiology, University Hospital Dubrava, Croatia. The images were characterized by an expert radiologist. The database comprises 72 cases, and each case includes CC and MLO views of left and right breast, i.e. four images per case. Each image in the database has a resolution of 4084 × 3328 pixels with 12 bits per pixel. All images were

stored in compliance with the DICOM standard. We have selected 6 mammographic image pairs in MLO view with bilateral asymmetry available in the KBD-FER database and randomly selected 20 normal mammographic image pairs in MLO view. We have reduced all images to the resolution of 0.2 x 0.2 mm and cropped/padded them so that every image has 1024 × 1024 pixels. Image segmentation was not necessary since there are no background artifacts in these digital images.

In the preprocessing step all right breast images were flipped in order to have the same orientation as the corresponding left breast image, and all images were converted to NIFTI (Neuroimaging Informatics Technology Initiative) format for use in the IRTK registration software.

V. RESULTS

We have validated the registration using six different measures:

- sum of squared differences (SSD)
- normalized cross correlation (NCC)
- mutual information (MI)
- normalized mutual information (NMI)
- structural similarity index (SSIM)
- universal image quality measure (UIQI)

The sum of squared differences (SSD), which was used as a similarity measure to lead the registration, was explained above in Section II. Values of SSD are higher when the difference between images is bigger.

Normalized cross correlation (NCC) [27] is defined as

$$NCC = \left| \frac{\sum_{m,n} \left(s(m,n) - \mu_x\right) \cdot \left(r(m,n) - \mu_y\right)}{\sqrt{\left(\sum_{m,n} \left(s(m,n) - \mu_x\right)^2\right)\left(\sum_{m,n} \left(r(m,n) - \mu_y\right)^2\right)}} \right| \quad (4)$$

where $s(m,n)$ and $r(m,n)$ are the intensities of the original and transformed image, and μ_x and μ_y are mean of the original and the transformed image. The maximal value that NCC can achieve is 1 which would imply that the images are in alignment.

Mutual information (MI) is defined as

$$MI(A,B) = H(A) + H(B) - H(A,B) = -\sum_a \sum_b p_{AB}(a,b) \log \frac{p_{AB}(a,b)}{p_A(a)\, p_B(b)} \quad (5)$$

where p_A and p_B are the marginal probability distributions, which can be thought of as the projection of the joint probability distribution function onto the axes corresponding to intensities in images A and B, respectively [19]. Mutual information is a measure of how well one image explains the other and is at maximum at the optimal alignment. When two images are entirely different, mutual information is zero. The maximum value of MI is 1.

Studholme et al. [23] showed that mutual information is not independent of the overlap of the two images. Thus, the use of normalized mutual information (NMI) is proposed and expressed as

$$NMI(A,B) = \frac{H(A) + H(B)}{H(A,B)} \quad (6)$$

which is more robust than mutual information. Values of NMI are in the range between 1 and 2, where value 1 denotes images that are entirely different and value 2 denotes that the images are identical.

The structural similarity index (SSIM) proposed by Wang et al. [28] is defined as

$$SSIM(x,y) = \frac{(2\mu_x\mu_y + C_1)(2\sigma_{xy} + C_2)}{(\mu_x^2 + \mu_y^2 + C_1)(\sigma_x^2 + \sigma_y^2 + C_2)} \quad (7)$$

where μ_x and μ_y are mean intensities of the first and the second image, σ_x and σ_y are standard deviations of the first and the second image, σ_{xy} is the covariance of the two images and C_1 and C_2 are constants in order to avoid instability. The SSIM index is in the range between 0 (different images) and 1 (identical images).

Universal image quality measure (UIQI) [29] models distortion as a combination of three factors: loss of correlation, luminance distortion and contrast distortion. It is defined as

$$UIQI = \frac{4\sigma_{xy}\mu_x\mu_y}{(\sigma_x^2 + \sigma_y^2)\left[(\mu_x)^2 + (\mu_y)^2\right]} \quad (8)$$

where μ_x and μ_y are mean intensities of the first and the second image, σ_x and σ_y are variances of the first and the second image, σ_{xy} is the covariance of the two images. The range of UIQI is [-1, 1], where the best value 1 is achieved when the images are identical.

The validation of the registration results using above mentioned measures is presented in Tables I, II and III. Values in the tables are mean values for each measure in the observed dataset before and after rigid registration of the mammographic images. Table I presents results of registration of images from the mini-MIAS dataset, Table II presents results of registration of images from the DDSM dataset and Table III presents results of registration of images from the KBD-FER dataset. From the results it can be concluded that registration overall works well on all three datasets with some exceptions depending on the measure used. Results also indicate that these measures might be used as a discriminator between normal and asymmetric tissue since normal cases mostly show higher similarity than asymmetric cases.

Fig. 1 shows an example from the mini-MIAS dataset: the original left image (Fig. 1 a), the original right image (Fig. 1 b), the difference image between left and right image before registration (Fig. 1 c), and the difference image between left and right image after rigid registration (Fig. 1 d).

Fig. 2 shows an example from the DDSM dataset: the original left image (Fig. 2 a), the original right image (Fig. 2 b), the difference image between left and right image before registration (Fig. 2 c), and the difference image between left and right image after rigid registration (Fig. 2 d).

Fig. 3 shows an example from the KBD-FER dataset: the original left image (Fig. 3 a), the original right image (Fig. 3 b), the difference image between left and right image before registration (Fig. 3 c), and the difference image between left and right image after rigid registration (Fig. 3 d).

In Figs. 1, 2 and 3 images have been cropped for the presentation purposes due to the limited space.

TABLE I. REGISTRATION RESULTS FOR THE MINI-MIAS DATASET

mini-MIAS		SSD	NCC	MI	NMI	SSIM	UIQI
asymmetric cases	before	797.01	0.9275	0.8567	1.1871	0.8431	0.5889
	after	726.78	0.9345	0.9108	1.2040	0.8557	0.6031
normal cases	before	765.66	0.9237	0.7983	1.2080	0.8678	0.6699
	after	598.41	0.9383	0.8741	1.2350	0.8875	0.6893

TABLE II. REGISTRATION RESULTS FOR THE DDSM DATASET

DDSM		SSD	NCC	MI	NMI	SSIM	UIQI
asymmetric cases	before	641.08	0.9365	0.7826	1.2163	0.8889	0.6912
	after	877.52	0.9037	0.8317	1.2452	0.9018	0.7041
normal cases	before	562.86	0.9512	0.9040	1.2237	0.8899	0.6493
	after	735.68	0.9343	0.9747	1.2544	0.9106	0.6758

TABLE III. REGISTRATION RESULTS FOR OUR KBD-FER DATASET

KBD-FER		SSD	NCC	MI	NMI	SSIM	UIQI
asymmetric cases	before	4.90×10^4	0.9462	0.4695	1.6340	0.7173	0.7012
	after	5.51×10^4	0.9417	0.4892	1.6963	0.7301	0.7139
normal cases	before	4.94×10^4	0.9428	0.4554	1.6321	0.7173	0.7011
	after	3.69×10^4	0.9511	0.4891	1.7212	0.7375	0.7205

VI. CONCLUSIONS

In the presented work we have used rigid registration to align mammographic images of the left and right breast as a first step in bilateral asymmetry analysis and detection which will be part of our future research. We have tested rigid registration on three datasets formed out of three different databases: the mini-MIAS and DDSM, which are publicly available databases with digitised images, and our KBD-FER database with digital mammographic images. Registration was validated using six different measures, which all showed that registration increases the similarity between images. Mean values of measures also revealed differences between asymmetric and normal cases which might lead to a conclusion that these measures might be used as a discriminative features between asymmetric and normal cases which will be considered in our future research.

ACKNOWLEDGMENT

The work in this paper was conducted under the research project "Intelligent Image Features Extraction in Knowledge Discovery Systems" (036-0982560-1643), supported by the Ministry of Science, Education and Sports of the Republic of Croatia.

The work in this paper was supported by the British Scholarship Trust, which is gratefully acknowledged.

The Image Registration Toolkit was used under Licence from Ixico Ltd.

REFERENCES

[1] American College of Radiology (ACR): ACR Breast Imaging Reporting and Data System, Breast Imaging Atlas, 4th Edition, Reston, VA, USA, 2003

[2] T.-K. Lau, W. F. Bischof, "Automated Detection of Breast Tumors Using the Asymmetry Approach", Computers and Biomedical Research, Vol. 24, No. 3, 1991, pp. 273-295

[3] F.-F. Yin, M. L. Giger, K. Doi, C. J. Vyborny, R. A. Schmidt, "Computerized Detection of Masses in Digital Mammograms: Automated Alignment of Breast Images and its Affect on Bilateral-Subtraction Technique", Medical Physics, Vol. 21, No. 3, March 1994, pp. 445-452

[4] A. J. Méndez, P. G. Tahoces, M.J. Lado, M. Souto, J. J. Vidal, "Computer-Aided Diagnosis: Automatic Detection of Malignant Masses in Digitized Mammograms", Medical Physics, Vol. 25, No. 6, June 1998, pp. 957-964

[5] M. A. Wirth, C. Choi, A. Jennings, "A Nonrigid-Body Approach to Matching Mammograms", Seventh International Conference on Image Processing and Its Applications, Manchester, UK, July 1999, pp. 484-488

[6] F. Georgsson, "Differential analysis of bilateral mammograms", International Journal on Pattern Recognition and Artificial Intelligence, Vol. 17, July 2003, pp. 1207-1226

[7] X. Wang, D. Lederman, J. Tan, X. H. Wang, B. Zheng, "Computerized Prediction of Risk for Developing Breast Cancer Based on Bilateral Mammographic Breast Tissue Asymmetry", Medical Engineering and Physics, 2011, in press, doi: 10.1016/j.medengphy.2011.03.001

[8] P. Miller, S. Astley, "Detection of Breast Asymmetry Using Anatomical Features", in: R.S. Acharya, C.B. Goldgof (Eds.), Biomedical Image Processing and Biomedical Visualization, Proceedings of SPIE, Vol. 1905, 1993, pp. 433-442

[9] P. Miller, S. Astley, "Automated detection of breast asymmetry using anatomical features", in: K.W. Bowyer, S. Astley (Eds.), State of the Art in Digital Mammographic Image Analysis, Series in Machine Perception and Artificial Intelligence, Vol. 9, World Scientific, River Edge, NJ, 1994, pp. 247-261

[10] D. Tahmoush, H. Samet, "Image Similarity and Asymmetry to Improve Computer-Aided Detection of Breast Cancer", Proceedings of the International Workshop on Digital Mammography (IWDM) 2006, Manchester, UK, June 2006, pp. 221-228

[11] R. M. Rangayyan, R. J. Ferrari, A. F. Frere, "Analysis of Bilateral Asymmetry in Mammograms Using Directional, Morphological, and Density Features", Journal of Electronic Imaging, Vol. 16, No. 1, January-March 2007, 013003-(1-12)

[12] N. Vujovic, D. Brzakovic, "Establishing the Correspondence Between Control Points in Pairs of Mammographic Images", IEEE Transactions on Image Processing, Vol. 6, No. 10, October 1997, pp. 1388-1399

[13] K. Marias, C. Behrenbruch, S. Parbhoo, A. Seifalian, Michael Brady, "A Registration Framework for the Comparison of Mammogram Sequences", IEEE Transactions on Medical Imaging, Vol. 24, No. 6, June 2005, pp. 782-790

[14] S. Timp, N. Karssemeijer, "Interval Change Analysis to Improve Computer Aided Detection in Mammography", Medical Image Analysis, Vol. 10, No. 1, February 2006, pp. 82-95

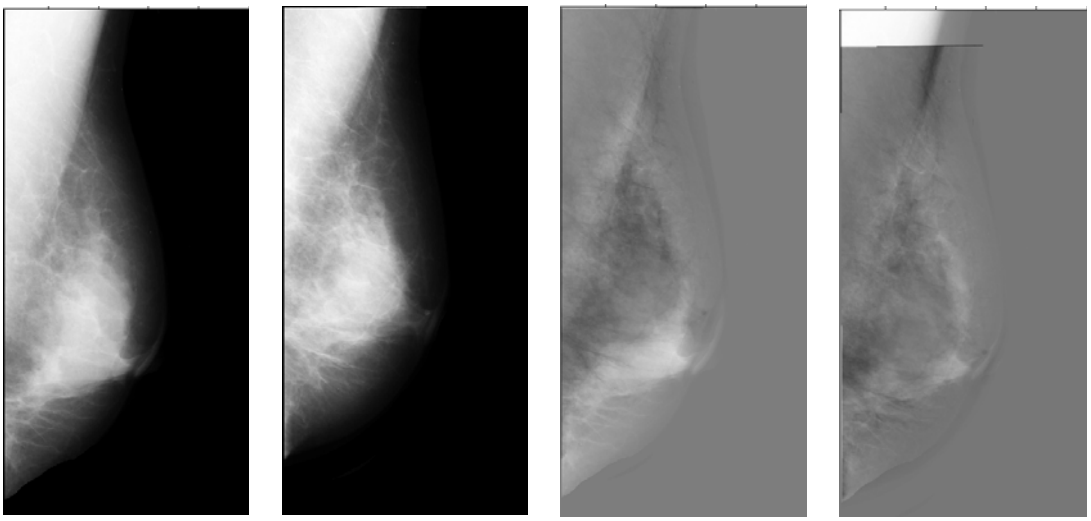

(a) (b) (c) (d)

Figure 1. An example from mini-MIAS dataset: (a) original left image, (b) original right image, (c) difference image before registration and (d) difference image after rigid registration

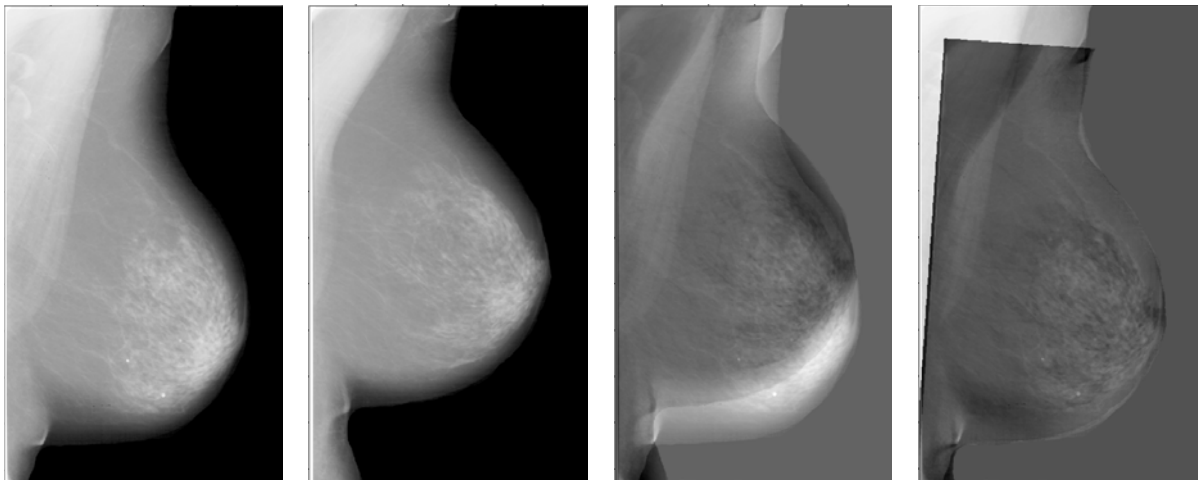

(a) (b) (c) (d)

Figure 2. An example from DDSM dataset: (a) original left image, (b) original right image, (c) difference image before registration and (d) difference image after rigid registration

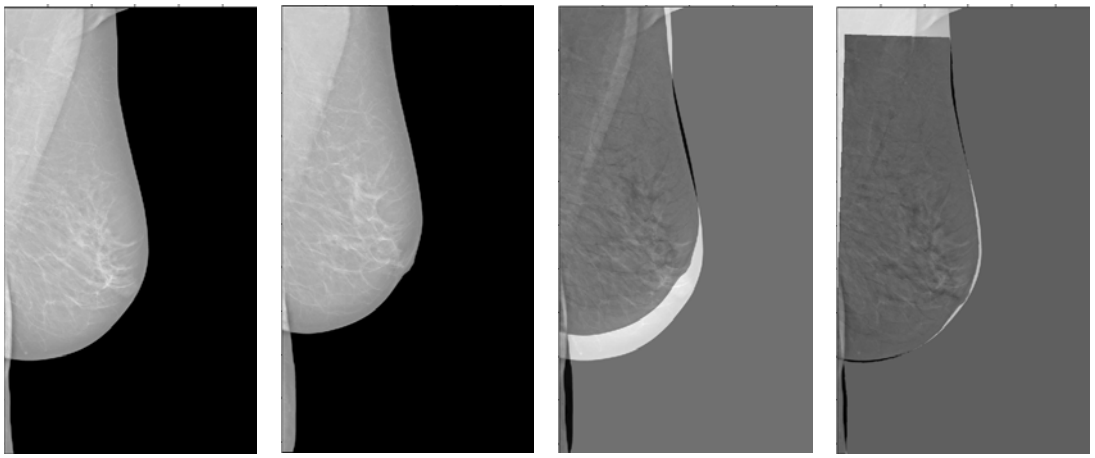

(a) (b) (c) (d)

Figure 3. An example from KBD-FER dataset: (a) original left image, (b) original right image, (c) difference image before registration and (d) difference image after rigid registration

[15] F. J. P. Richard, P. R. Bakic, A. D. A. Maidment, "Mammogram Registration: A Phantom-Based Evaluation of Compressed Breast Thickness Variation Effects", IEEE Transactions on Medical Imaging, Vol. 25, No. 2, February 2006, pp. 188-197

[16] Y. Guo, R. Sivaramakrishna, C.-C. Lu, J. S. Suri, S. Laxminarayan, "Breast Image Registration Techniques: A Survey", Medical and Biological Engineering and Computing, Vol. 44, 2006, pp. 15–26

[17] S. van Engeland, P. Snoeren, J. Hendriks, N. Karssemeijer, "A Comparison of Methods for Mammogram Registration", IEEE Transactions on Medical Imaging, Vol. 22, No. 11, November 2003, pp. 1436-1444

[18] M. A. Wirth, J. Narhan, D. Gray, "Nonrigid Mammogram Registration Using Mutual Information", SPIE Medical Imaging: Image Processing, San Diego, USA, Vol. 4684, February 2002, pp.562-573

[19] J. V. Hajnal, D. Hill, D. J. Hawkes, Medical Image Registration, CRC Press LLC, Boca Raton, 2001

[20] H. F. G. García, A. G. Vega, A. H. Aguirre, J. L. M. Zaleta, C. A. C. Coello, "Robust Multiscale Affine 2D-Image Registration through Evolutionary Strategies", PPSN VII Proceedings of the 7th International Conference on Parallel Problem Solving from Nature, Granada, Spain, September 2002, pp. 740-748

[21] D. L. G. Hill, P. G. Batchelor, M. Holden, D. J. Hawkes, Medical Image Registration, Physics in Medicine and Biology, Vol. 46, pp. R1–R45, 2001

[22] Image Registration Toolkit IRTK, Available at: www.doc.ic.ac.uk/~dr/software

[23] C. Studholme, D. L. G. Hill, D. J. Hawkes, "An Overlap Invariant Entropy Measure of 3D Medical Image Alignment", Pattern Recognition, Vol. 32, No. 1, January 1999, pp. 71-86

[24] J. Suckling, J. Parker, D. Dance et al., "The Mammographic Image Analysis Society Digital Mammogram Database", Exerpta Medica, International Congress Series 1069, 1994, pp. 375-378

[25] M. Heath, K. Bowyer, D. Kopans, R. Moore, W. P. Kegelmeyer, "The Digital Database for Screening Mammography", Proceedings of the Fifth International Workshop on Digital Mammography, Medical Physics Publishing, 2001, pp. 212-218

[26] M. Heath, K. Bowyer, D. Kopans, W. P. Kegelmeyer, R. Moore, K. Chang, S. M. Kumaran, "Current status of the Digital Database for Screening Mammography", Proceedings of the Fourth International Workshop on Digital Mammography, Kluwer Academic Publishers, 1998, pp. 457-460

[27] T. M. Lehman, C. Gönner, K. Spitzer, "Survey: Interpolation Methods in Medical Image Processing", IEEE Transactions on Medical Imaging, Vol. 18, No. 11, November 1999, pp. 1049-1075

[28] Z. Wang, A. C. Bovik, H. R. Sheikh, E. P. Simoncelli, "Image Quality Assessment: From Error Visibility to Structural Similarity", IEEE Transactions on Image Processing, Vol. 13, No. 4, pp. 600-612, April 2004

[29] Z. Wang, A. C. Bovik, "A Universal Image Quality Index", IEEE Signal Processing Letters, Vol. 9, No. 3, March 2002, pp. 81-84